Optics Letters

Chirped flicker optoretinography for *in vivo* characterization of human photoreceptors' frequency response to light

Sławomir Tomczewski,[1,2] Piotr Węgrzyn,[1,2,3] Maciej Wojtkowski,[1,2,*] and Andrea Curatolo[1,2,4]

[1] International Centre for Translational Eye Research, Skierniewicka 10A, 01-230, Warszawa, Poland
[2] Institute of Physical Chemistry, Polish Academy of Sciences, Kasprzaka 44/52, 01-224 Warszawa, Poland
[3] Faculty of Physics, University of Warsaw, Pasteura 5, 02-093 Warszawa, Poland
[4] Department of Physics, Politecnico di Milano, Piazza Leonardo da Vinci 32, 20133 Milan, Italy
*mwojtkowski@ichf.edu.pl

Received 29 November 2023; revised 28 March 2024; accepted 2 April 2024; posted 3 April 2024; published 30 April 2024

Flicker electroretinography (ERG) has served as a valuable noninvasive objective tool for investigating retinal physiological function through the measurement of electrical signals originating from retinal neurons in response to temporally modulated light stimulation. Deficits in the response at certain frequencies can be used as effective biomarkers of cone-pathway dysfunction. In this Letter, we present the progress we made on its optical counterpart—photopic flicker optoretinography (f-ORG). Specifically, we focus on the measurement of the response of light-adapted retinal photoreceptors to a flicker stimulus with chirped frequency modulation. In contrast to measurements performed at discrete frequencies, this technique enables a significantly accelerated characterization of photoreceptor outer segment optical path length modulation amplitudes in the nanometer range as a function of stimulus frequency, enabling the acquisition of the characteristic frequency response in less than 2 sec.

https://doi.org/10.1364/OL.514637

In many ocular diseases, there is a complex structure–function relationship [1]. Moreover, the time lag between functional deficits and detectable pathological changes in ocular morphology is also variable and not easily determined [2]. In ophthalmic research and practice, psychophysical and electrophysiological methods are used to obtain information on visual function. Psychophysical tests, e.g., microperimetry [3], or flicker sensitivity tests [4] are subjective as they rely on the answers from the test subject detecting and visually processing the light stimulus. Visual electrophysiology tests, such as electroretinography (ERG) [5], measure changes in electric potentials originating from retinal neurons in response to light stimulation. They are mildly invasive, objective tests that require the installation of special electrodes on the test subject.

Flicker ERG is a type of ERG measurement of the retinal response to a flickering stimulus [6]. The frequency response characteristics of the ERG signals have been studied extensively by Burns and Elsner, both at low temporal frequencies [7] and at higher frequencies, where they exhibit non-linearities. These frequency response studies proved to be instrumental in the analysis of retinal light adaptation [8] and critical flicker frequency (CFF). In humans, studies of the frequency response ERG have highlighted its potential as a biomarker of early development of retinitis pigmentosa [9], of X-linked retinoschisis [10], and of diabetic retinopathy [11], with attenuated high-frequency responses in diseased subjects.

In recent years, it has been shown that retinal imaging techniques such as adaptive optics scanning laser ophthalmoscopy and optical coherence tomography (OCT) could detect small changes in reflected infrared (IR) light intensity occurring after simultaneous stimulation with visible light, laying the foundations for optoretinography (ORG), a group of techniques that measure light-evoked changes in the photoreceptor layer or even in individual cells [12].

With OCT, these signals can be derived from intensity-based measurements (iORG) [13] or phase-based optoretinograms (pORG) [14]. Many ORG studies focused on the photoreceptor outer segment (OS) length change as a functional response to a single light flash bleaching some photopigments, giving rise to theories about the potential origin of the response as the physical manifestation of the first steps of phototransduction and osmotic balance restoration, depending on the time delay from the stimulus onset [15,16].

Similarly to photopic flicker electroretinography, we recently have performed f-ORG experiments with humans to measure the OS response of the photoreceptors to a flicker stimulus under light-adapted conditions (photopic) over a broad range of stimulus frequencies [17]. In our work, we noticed that changes in optical path length of the cone outer segment, i.e., between the inner and outer segment junction and the cone outer segment

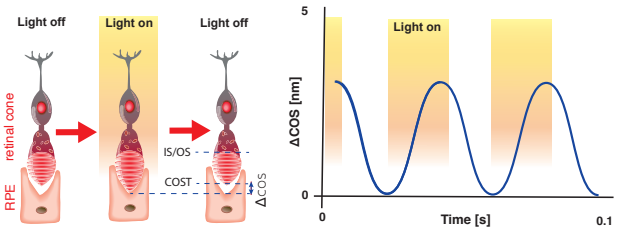

Fig. 1. Simplified representation of the effect of flickering light on the cone's outer segment; RPE, retinal pigment epithelium.

tips, from its length after light-adaptation (ΔCOS) oscillate with the frequency of the stimulus (Fig. 1).

The light-adapted flicker protocol has two benefits. On the one hand, it enables the measurement of optical path length modulation amplitudes with better signal-to-noise ratios than for dark-adapted eyes as it enables recording of flicker-induced optical path length modulation over a steady background during the whole acquisition window [17]; and on the other hand, it allows for a decrease in measurement time by avoiding several minutes of dark adaptation [18].

Unfortunately, performing full frequency characterization requires an extensive number of measurements at separate stimulus frequencies and conducting time-consuming data processing for each of the acquired datasets. In this Letter, we use frequency-chirped stimulus in f-ORG, enabling clinically viable frequency response characterization of photoreceptors. The frequency sweep protocol has been previously used in ophthalmology for measurements of critical flicker frequency (CFF) with the use of ERG [19], and it gave results in agreement with measurements at separate stimulus frequencies.

To record chirped f-ORG signal, we use a spatiotemporal optical coherence tomography (STOC-T) setup described in detail in previous reports [17,20]. For the stimulation, we use a white LED, with a central wavelength of 550 nm and a FWHM bandwidth of 260 nm. The spectral shape of the LED, measured at the eye pupil plane, was presented in our previous work (Fig. 1 in [17]). The measured rise and fall times of the LED were 3 and 1 ms, respectively. The retina was stimulated with a linearly chirped signal (from 5 to 45 Hz, sweep rate of 22.2 Hz/s), and we record 340 spectral volumes (256 × 256 camera pixels × 512 images) at a volume repetition rate of 188 Hz. During the flicker stimulation, the illuminance on the retina repeatedly changed from 0 Td (excluding the illuminance of the OCT beam) to a maximum value (specified in the description of each experiment as the peak illuminance). For the reference measurements at separate stimulus frequencies, we record a set of 170 volumes (512 × 256 camera pixels × 512 images) at a volume repetition rate of 188 Hz, for stimulus frequencies every 5 Hz. In this case, for each separate flicker-frequency measurement, the acquisition time is approximately 0.9 sec, while the time required to acquire all data points for characterization of the full photoreceptor-frequency response is several minutes. The measurement time for the chirped f-ORG acquisition is instead approximately 1.8 sec. In the case of separate flicker-frequency measurements, we usually perform three acquisitions at every given frequency to have meaningful data, while in the chirped stimulus, cases around five acquisitions are enough for the whole characteristics. However, the numbers might differ depending on the subject's stability and quality of STOC-T signal.

To retrieve the f-ORG signal, we processed the data, using the procedure described in detail in our previous report [17]. However, STOC-T images can suffer from artifacts due to fast transverse eye movements occurring within the laser sweep. Given the small temporal window for each short-time Fourier transform, it is essential to retain as many good-quality STOC-T volumes as possible. To correct for such artifacts, we modified a windowing approach, previously applied to the correction of axial movements in FF-FD-OCT systems [21]. For each spectral volume, we divide the spectrum into eight 64-point subspectra. Then these sub-spectra are Fourier transformed to obtain low axial resolution volumes; and transverse shifts between these volumes required for their alignment are computed by performing their cross correlation in Fourier space. Finally, a spline interpolation is applied to the calculated shift values, and transverse shift correction is applied to each interferogram.

The complete single measurement data processing using MATLAB scripts (340 OCT volumes, 512 × 256 × 256 pixels) takes approximately 48 min on a 3-year-old PC (AMD Ryzen 3900X, GeForce 3060, 128 GB of RAM).

Figure 2(a) shows an example of the measured change in the optical path length between IS/OS and COST, from the starting length, i.e., DeltaCOS length (averaged from seven measurement repetitions and after filtering out low frequencies for better presentation) with linear frequency-chirped square wave flicker stimulation illuminating the retina (shaded area). In the last step, we analyze such signals using a short-time Fourier transform (computed using a window size $W = 48$ volumes and an overlap $O = 24$ volumes) to obtain spectrograms describing the frequency content of the optical path length modulation amplitude from 7.7 to 42.2 Hz, in consecutive time bins (I–XIII). Lastly, the spectrograms from all repetitions are averaged [see Fig. 2(b)], and the response amplitudes at the center frequencies corresponding to each time bin are extracted to form the frequency response characteristics. Though the signal averaging leads to a response that seems buried in the noise above 1.2 sec in Fig. 2(a), the spectrogram averaging in Fig. 2(b) shows that the response is above the noise level within the whole measurement range.

To experimentally validate chirped f-ORG, we performed a set of *in vivo* experiments. All presented research was approved by the Bioethical Committee at the Ludwik Rydygier Collegium Medicum of Nicolaus Copernicus University (approval KB 87/2021). It was conducted following the tenets of the Declaration of Helsinki. The STOC-T imaging beam power at the cornea was equal to 3.9 mW. The safety of working with the tunable laser (Broadsweeper 840-2-HP, Superlum) has been evaluated in detail, as described in our previous publication [20]. Four volunteers with no known pathologies were recruited for this study. After the nature and possible risks of the study were explained, the subjects provided informed consent. Only the subjects' right eyes were used, and the subjects' pupils were not dilated for the experiments. All the measurements were performed in a retinal region 5° nasal to the fovea, and the responses were averaged from the whole field of view (FOV), which was 0.85 × 0.85 mm in the case of chirped f-ORG. The illuminated retinal area was larger than FOV to keep the whole FOV stimulated even in case of eye movements.

Before the start of flicker and data acquisition, the retina of each subject was adapted to light [17]. In the first set of experiments, the 60 sec light adaptation with 47 μW (110,000 photopic Td) bleached ~ 81% of the cone-photoreceptor pigment. The

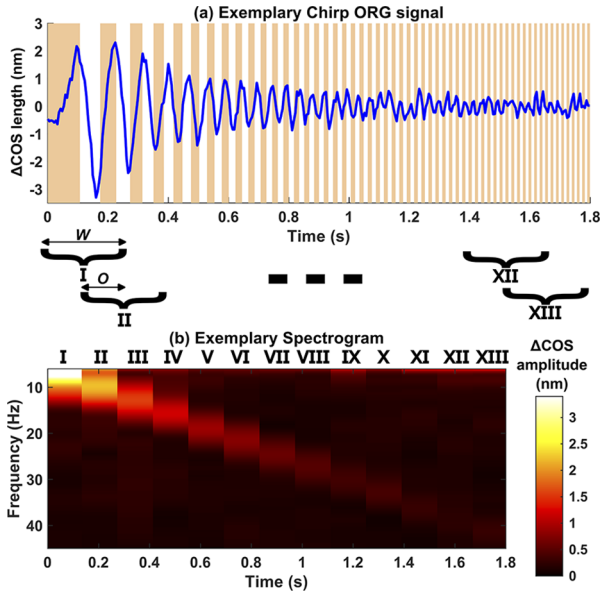

Fig. 2. Example results from f-ORG measurements. (a) Linear frequency-chirped stimulation illuminating the retina (shaded areas) and the corresponding f-ORG signal (averaged from seven repeated measurements after filtering out low frequencies for better visualization). (b) Example of spectrogram computed by averaging spectrograms from all seven repetitions.

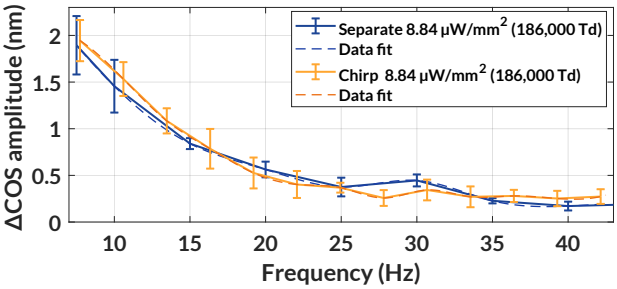

Fig. 3. Comparison of ΔCOS amplitudes measured separately at different flicker frequencies (blue) and with the frequency-chirped flicker stimulus (orange). Dashed lines represent fitted data used for error estimation.

retinal illuminance in Td and bleach values were calculated as in our previous paper [17]. We then used a peak retinal illuminance of 186,000 Td during the flicker stimulation and compared the results from the frequency-chirped flicker stimulus (five repetitions) with the results from a constant-frequency flicker repeated at different frequencies (32 measurements in total), as described above. Figure 3 shows that both curves largely overlap. To numerically quantify the difference between the results of the two procedures, first we fitted spline curves to the measured frequency responses due to different frequency samplings. A spline was selected as it can closely follow the irregularities in the plots. Then we computed the RMS difference, equal to 96 pm, and the maximum difference, equal to 170 pm, between fitted curves.

In further experiments, the light adaptation and flicker illuminances were reduced. These changes increased the comfort level of the subjects and resulted in a higher success rate (less vignetting on the eye iris and increased stability during flicker).

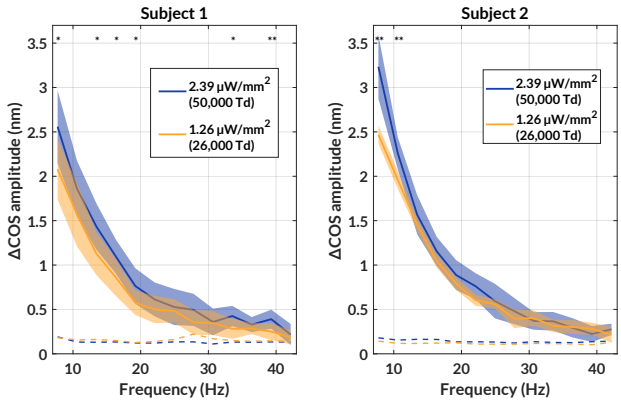

Fig. 4. Comparison of ΔCOS amplitudes in two subjects for two different peak retinal illuminance. The glow represents the standard deviation, and the asterisks mark the significant differences: * - p-value < 0.05; ** - p-value < 0.01. Dashed lines represent the corresponding noise floor.

The 60 sec light adaptation with 15 μW (35,000 Td) bleached ~41% of the cone-photoreceptor pigment. In the second set of experiments, we investigated whether the flicker ORG can detect significant differences in cone OS responses under two different peak flicker illuminances (50,000 and 26,000 Td). The frequency characteristics we obtained are presented in Fig. 4. The noise floor values at each data point on the frequency axis were obtained by calculation of the RMS value of the corresponding column of the averaged spectrogram (in the 7.75–42.25 Hz range, excluding a 10 Hz wideband around the stimulus frequency). We observed lower cone OS optical path length modulation amplitudes for the lower retinal illuminance case quite consistently across the frequency range, for subject 1, while mainly below 12 Hz, for subject 2. In the last set of experiments, we compared the response to a frequency-chirped square wave stimulus with the response to a frequency-chirped sinusoidal stimulus. The frequency characteristics are presented in Fig. 5, where the response to a square wave stimulus is larger than the response to a sinusoidal stimulus, especially at lower frequencies. Lastly, we measured two additional subjects (using a peak illuminance of 50,000 Td for the chirped square wave flicker stimulus), and we compared the results for this small group (Fig. 6). For three subjects, the amplitudes of the frequency response were similar, while one subject had a higher average response amplitude below 15 Hz.

Interestingly, the general monotonically decreasing shape of the frequency characteristics of the cone OS optical path length modulation amplitude differs from the frequency response of the ERG signal, which for healthy humans often shows a peak around 30 Hz [7]. Some of the significant differences observed in the first subject above 30 Hz in both experiments might be artifactual. We think that this is the case, especially for the chirped square wave flicker stimulus with 50,000 Td peak illuminance. Investigation of ORG signals suggests that spurious phase difference modulation was caused by the COS length change estimation step that used a simple STOC-T phase difference evaluation between consecutive time points. The use of more advanced methods, such as the Knox–Thompson method [22], might improve the quality of the results.

We hypothesize that the lack of a 30 Hz maximum in the f-ORG plots is related to the different origins of the signal. The

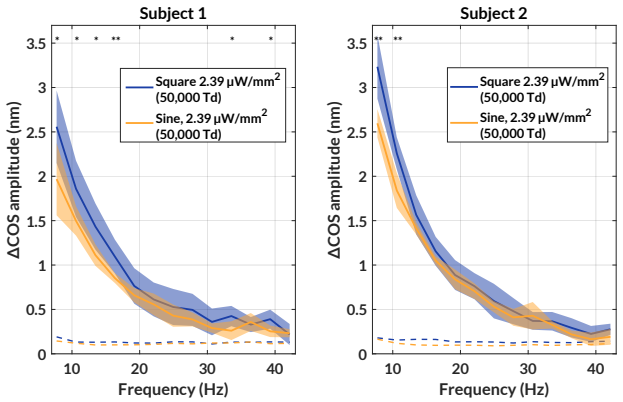

Fig. 5. Comparison of ΔCOS amplitudes between square wave and sinusoidal chirped stimuli in two subjects. Dashed lines represent the corresponding noise floor.

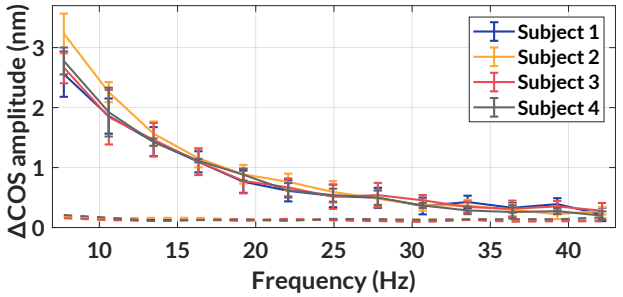

Fig. 6. Comparison of ΔCOS amplitudes in four subjects under the same stimulus conditions (see text). Error bars represent ± one standard deviation. Dashed lines represent the corresponding noise floor.

flicker ERG measures electric signals from the whole cone pathway, and dominance of the postreceptoral component is maximal at 30 Hz [23], while our f-ORG focuses only on the changes in the optical path length within the cones' outer segment.

Meanwhile, we think that the difference between responses to the sinusoidal and square wave stimuli of the same amplitude is the result of $4/\pi$ times higher amplitude of the fundamental component of the square waveform. Such differences must be taken into account when comparing results obtained with different stimulus types.

Though subject 2 differed from the rest of the group in a number of features, we prefer to avoid speculations on their correlation and/or causality to the differences without performing measurements on a larger group of subjects.

The implementation of frequency chirp to our f-ORG stimulus significantly reduces the number of measurements needed to characterize the photoreceptors' frequency response, drastically lowering the time required to perform the experiments and analyze the data. We have shown that there are no significant differences between sequential reading and chirp stimulation. Reducing the illuminance of the flashing stimulus causes significant changes in the amplitude of the photoreceptor response in the frequency region from 7 to 30 Hz, indicating the frequency range optimal for sensitive f-ORG recording. For a precise measurement of the frequency characteristics, we suggest an accurate selection of the pre-flicker illuminance for adaptation and the flicker mean illuminance, to avoid drifts in ΔCOS at the beginning of the flicker stimulation. Given the limited number of subjects and measurements, the significant differences presented herein should be considered preliminary and necessitate further research. Future experiments will focus on studying f-ORG frequency responses at different eccentricities and with varying modulation contrasts. Ultimately, this approach may provide a frequency response-based biomarker for early detection of retinal degeneration and ORG-enabled monitoring of therapy.

Funding. National Science Center (2020/38/L/ST2/00556); The International Centre for Translational Eye Research (MAB/2019/12) is carried out within the International Research Agendas Programme of the Foundation for Polish Science, co-financed by the European Union under the European Regional Development Fund.

Disclosures. The authors declare no conflicts of interest.

Data availability. Data underlying the results presented in this paper are not publicly available at this time, but may be obtained from the authors upon reasonable request.

REFERENCES

1. J. Phu, M. Kalloniatis, H. Wang, *et al.*, Front. Neurosci. **13**, 306 (2019).
2. S. K. Gardiner, S. L. Mansberger, and B. Fortune, Invest. Ophthalmol. Visual Sci. **61**, 5 (2020).
3. A. Molina-Martín, R. J. Pérez-Cambrodí, and D. P. Piñero, Semin. Ophthalmol. **33**, 620 (2018).
4. M. J. Mayer, C. B. Y. Kim, A. Svingos, *et al.*, J. Opt. Soc. Am. A **5**, 2201 (1988).
5. P. Gouras, Invest. Ophthalmol. Visual Sci. **9**, 557 (1970).
6. G. H. Jacobs, J. Neitz, and K. Krogh, J. Opt. Soc. Am. A **13**, 641 (1996).
7. S. A. Burns and A. E. Elsner, J. Opt. Soc. Am. A **13**, 667 (1996).
8. S. Wu and S. A. Burns, J. Opt. Soc. Am. A **13**, 649 (1996).
9. H. Hassan-Karimi, E. Jafarzadehpur, B. Blouri, *et al.*, J. Ophthalmic Vis. Res. **7**, 34 (2012).
10. K. R. Alexander, C. S. Barnes, and G. A. Fishman, Invest. Ophthalmol. Visual Sci. **42**, 2094 (2001).
11. J. J. McAnany, Y.-F. Chen, K. Liu, *et al.*, Vision Res. **161**, 1 (2019).
12. R. S. Jonnal, Ann. Transl. Med. **9**, 1270 (2021).
13. G. Ma, T. Son, T.-H. Kim, *et al.*, Biomed. Opt. Express **12**, 2661 (2021).
14. D. Hillmann, H. Spahr, C. Pfaffle, *et al.*, Proc. Natl. Acad. Sci. U. S. A. **113**, 13138 (2016).
15. V. P. Pandiyan, A. Maloney-Bertelli, J. A. Kuchenbecker, *et al.*, Sci. Adv. **6**, eabc1124 (2020).
16. V. P. Pandiyan, P. T. Nguyen, E. N. Pugh, *et al.*, Proc. Natl. Acad. Sci. U. S. A. **119**, e2202485119 (2022).
17. S. Tomczewski, P. Węgrzyn, D. Borycki, *et al.*, Biomed. Opt. Express **13**, 2186 (2022).
18. M. Kalloniatis and C. Luu, in *Webvision: The Organization of the Retina and Visual System*, H. Kolb, E. Fernandez, and R. Nelson, eds. (University of Utah Health Sciences Center Copyright: 2024 Webvision, 1995).
19. M. L. DeRamus and T. W. Kraft, in *Retinal Degenerative Diseases*, J. D. Ash, R. E. Anderson, M. M. LaVail, *et al.*, eds. (Springer International Publishing, 2018), pp. 145–150.
20. E. Auksorius, D. Borycki, P. Wegrzyn, *et al.*, iScience **25**, 105513 (2022).
21. D. Hillmann, T. Bonin, C. Lührs, *et al.*, Opt. Express **20**, 6761 (2012).
22. H. Spahr, C. Pfäffle, S. Burhan, *et al.*, Sci. Rep. **9**, 11748 (2019).
23. R. Verma and M. J. Pianta, Journal of Vision **9**, 9 (2009).